Available online at www.sciencedirect.com
ScienceDirect
Journal of Power Sources 160 (2006) 1369–1374
JOURNAL OF POWER SOURCES
www.elsevier.com/locate/jpowsour

Synthesis and electrochemical studies of the 4 V cathode, $Li(Ni_{2/3}Mn_{1/3})O_2$

M.V. Reddy, G.V. Subba Rao, B.V.R. Chowdari *

Department of Physics, National University of Singapore, Singapore 117542, Singapore

Received 20 December 2005; accepted 1 March 2006
Available online 15 May 2006

Abstract

Layered $Li(Ni_{2/3}Mn_{1/3})O_2$ compounds are prepared by freeze-drying, mixed carbonate and molten salt methods at high temperature. The phases are characterized by X-ray diffraction, Rietveld refinement, and other methods. Electrochemical properties are studied versus Li-metal by charge–discharge cycling and cyclic voltammetry (CV). The compound prepared by the carbonate route shows a stable capacity of 145 (±3) mAh g^{-1} up to 100 cycles in the range 2.5–4.3 V at 22 mA g^{-1}. In the range 2.5–4.4 V at 22 mA g^{-1}, the compound prepared by molten salt method has a stable capacity of 135 (±3) mAh g^{-1} up to 50 cycles and retains 96% of this value after 100 cycles. Capacity-fading is observed in all the compounds when cycled in the range 2.5–4.5 V. All the compounds display a clear redox process at 3.65–4.0 V that corresponds to the $Ni^{2+/3+}$–$Ni^{3+/4+}$ couple.

Keywords: $Li(Ni_{2/3}Mn_{1/3})O_2$; Layered structure; Cathode material; Lithium-ion battery; Capacity-fading; Electrochemical properties

1. Introduction

Lithium nickel–manganese oxides with a rhombohedral–hexagonal layer structure are being investigated as prospective, second-generation, 4 V cathode (positive electrode) materials to replace costly and toxic $LiCoO_2$ for use in Li-ion batteries (LIB) [1,2]. Specifically, Mn-substituted $LiNi^{3+}O_2$ compositions have been studied to suppress the capacity-fading exhibited by pure $LiNiO_2$ on repeated charge–discharge cycling. This effect involves the $Ni^{3+/4+}$ redox couple [3–5]. Recently, compounds of the type, $Li(Ni_xLi_{(1-2x)/3}Mn_{(2-x)/3})O_2$, $x < 1/2$ and $Li(Ni_{1/2}Mn_{1/2})O_2$ ($x = 1/2$) have attracted much attention [6–12]. This is due to the fact that Ni^{2+} ions in these compounds are electrochemically active and contribute to the reversible cathodic capacity through both $Ni^{2+/3+}$ and $Ni^{3+/4+}$ redox couples. The Mn^{4+} ions are tetravalent and play a beneficial role by stabilizing the layer structure and ensuring good electronic conductivity. On the other hand, Mn^{4+} ions in the above compounds are not electrochemically active in the voltage region of interest, viz., 3.5–4.5 V versus Li (metal).

Kobayashi et al. [13] reported the crystal structure, physical properties and preliminary electrochemical behaviour of $Li(Ni_{1-x}Mn_x)O_2$ phases and found that for x in the range 0.2–0.5, the compounds can be prepared by mixing and heating the raw materials in air at high temperatures. In addition, XANES and magnetic susceptibility data show that for $x = 0.2$–0.5, only Mn^{4+} ions are present, whereas both Ni^{2+} and Ni^{3+} ions exist in suitable proportions depending on the value of x, to ensure chargeneutrality in $Li(Ni_{1-x}Mn_x)O_2$ [13]. The composition, $Li(Ni_{2/3}Mn_{1/3})O_2$ is of particular interest since it contains equal amounts of Ni^{2+} and Ni^{3+} ions. Both these ions are electrochemically active and can contribute to the reversible capacity in the 4-V region. Further, the mixed valent ions can ensure good electronic conductivity of the mixed oxide. In the present study, $Li(Ni_{2/3}Mn_{1/3})O_2$ compounds are prepared by three methods and their cathodic properties versus Li-metal are examined. The results show that the compound acts as a good 4 V cathode.

2. Experimental

The $Li(Ni_{2/3}Mn_{1/3}O_2$ powder was synthesized by freeze-drying and mixed carbonate precursor methods, and also by using molten salts. In the freeze-drying method, stiochiomet-

* Corresponding author. Tel.: +65 6874 2956; fax: +65 6777 6126.
E-mail address: phychowd@nus.edu.sg (B.V.R. Chowdari).

0378-7753/$ – see front matter © 2006 Published by Elsevier B.V.
doi:10.1016/j.jpowsour.2006.03.046

ric amounts of LiOH (Merck), $Ni(CH_3COO)_2{\cdot}4H_2O$ (Merck) and $Mn(CH_3COO)_2{\cdot}4H_2O$ (Merck) were dissolved separately in de-ionized water, mixed in a beaker, and cooled with liquid nitrogen. The solid product was then freeze-dried at −20 °C using a Labconco, Freezone 4.5, USA unit. The resulting product was ground and heated at 300 °C for 5 h in air in a box furnace (Carbolite, UK) to decompose the acetates, and cooled to room temperature. The product was ground in an auto grinder, pressed in to pellets, and heated at 480 °C for 5 h and then at 900 °C for 24 h in air. The pellets were cooled to room temperature and thoroughly ground to a fine powder.

The carbonate method involved the precipitation of nickel and manganese (II) nitrates as a mixed carbonate precursor. To a solution of Ni- and Mn-nitrates (0.67 and 0.33 mol), a 1.5 M solution of $NaHCO_3$ was added, drop by drop, with continuous stirring. The solution was kept at ∼90 °C by heating on a hot plate and CO_2 gas was bubbled to maintain the pH at 7–8. The solution was filtered and the precipitate was washed with de-ionized water to remove excess sodium salts and dried in an air oven at 120 °C. The mixed carbonate was heated in air at 600 °C for 48 h to convert it to a mixed oxide. It was then mixed with a stiochiometric amount of LiOH and pressed into pellets. The pellets were heated at 480 °C for 5 h and then at 900 °C (heating rate 3 °C min^{-1}) for 24 h in air and then cooled to room temperature by furnace shut-off. The pellets were ground to a fine powder.

Molten salt synthesis involved mixing $LiNO_3$ (11.22 g, Alfa Aesar) and LiCl (0.941 g, Merck) salts in the mole ratio 0.88:0.12 (eutectic composition) with $Ni(NO_3)_2{\cdot}6H_2O$ (8.966 g, Merck) and $Mn(NO_3)_2{\cdot}4H_2O$ (3.869 g, Merck) in the mole ratio 0.67:0.33. The total mole ratio of Ni and Mn nitrates versus the eutectic was kept at 1:4. The mixture was placed in an alumina crucible, heated in air at 3 °C min^{-1} up to 850 °C and then kept for 4 h at that temperature. After cooling to room temperature, the product was thoroughly washed with de-ionized water and decanted several times to remove excess lithium salts, and filtered. The residue was dried in an air oven at 120 °C for 24 h. A free-flowing, black powder (∼4.6 g) was obtained.

Powder X-ray diffraction (XRD) patterns were obtained with a D8 Bruker axs diffractometer and Cu Kα radiation. Rietveld refinement of the XRD data was preformed with TOPAS-R (version 2.1) software. The morphology of the powders was examined with a JEOL JSM-6700F scanning electron microscope (SEM). The Brunauer, Emmett and Teller (BET) surface area of the powder was measured by means of a Micromeritics Tristar 3000 (USA) unit and the density was determined with a AccuPyc 1330 pycnometer (Micromeritics, USA).

Electrodes were fabricated from the active material, a super P carbon black and a binder (Kynar 2801) in the weight ratio 80:10:10. *N*-methyl pyrrolidone (NMP) was used as a solvent during mixing to dissolve the binder. The slurry was then coated on an etched aluminum foil (15 μm thick; Alpha Industries, Japan) using the doctor blade technique to obtain a thick film (20–22 μm). Each electrode was dried in a vacuum oven at 70 °C, pressed between twin rollers, and cut into 16-mm diameter circular disks. Coin-type cells (size, 2016) were fabricated using this composite electrode as a cathode in an argon-filled glove box (MBrann, Germany), which maintained an atmosphere of ≤1 ppm of H_2O and O_2. Lithium metal foil (Kyokuto metal Co., Japan) was used as the negative electrode (anode), 1 M $LiPF_6$ in ethylene carbonate (EC) and diethyl carbonate (DEC) (1:1 (v/v)) (Merck) as the electrolyte, and a Celgard 2502 membrane as the separator. Details of fabrication have been reported elsewhere [12,14]. Charge–discharge cycling at constant current and cyclic voltammetry were carried out on the cells by means of a computer-controlled, multi-channel, battery tester (Model SCN, Bitrode, USA) and a Mac-pile II, system (Bio-logic, France). The cells were aged for 24 h prior to test and studies were carried out ambient temperature (25 °C), and at 50 °C by keeping the cells in an oven. Differential scanning calorimetry (DSC) was preformed with a DSC TA instrument (Model 2920, USA), at a heating rate of 5 °C min^{-1}.

3. Results and discussion

3.1. Structure and morphology

The use of a freeze-dried acetate-hydroxide precursor or a precipitated mixed (Ni, Mn)-carbonate precursor ensures atomic-scale mixing of the metal ions. Subsequent grinding/mixing, pelletizing and heat treatment at high temperature (900 °C) gives rise to the formation of the desired layer-type structure in the compounds. Similarly, digesting (Ni, Mn) salts in the proper ratio in a molten salt eutectic at 850 °C for 4 h assists the decomposition of metal nitrates to the oxides. Thorough mixing and subsequent reaction with lithium ions result in the formation of the compound, $Li(Ni_{2/3}Mn_{1/3})O_2$. The molten salt method of synthesis of mixed oxides has recently been applied to the preparation of LIB cathodes, e.g., $LiMn_2O_4$ [15] and $LiCoO_2$ [16–18]. While the $LiNO_3$ acts as an oxidizing agent to produce Ni^{3+} and Mn^{4+} ions, the LiCl in the eutectic serves as a 'mineralizer' to ensure good crystallinity of the resulting mixed oxide, $Li(Ni_{2/3}Mn_{1/3})O_2$. Further, due to the large excess of the Li-salt mixture, consumption of Li to form the compound will not affect the composition nor the low melting point of the eutectic, $0.88LiNO_3$:0.12 LiCl (280 °C [19]). Synthesis parameters such as temperature and time of digestion to form the desired compound have not been optimized in the present study.

The $Li(Ni_{2/3}Mn_{1/3})O_2$ compounds prepared by the three methods are black, crystalline, free-flowing powders. For convenience, compounds I, II and III refer to the phases prepared by the freeze-drying, mixed carbonate and molten salt methods, respectively. The XRD patterns are shown in Fig. 1. They are indexed on the basis of a hexagonal layered, $LiCoO_2$-type structure. Rietveld refinement of the XRD data of compound III was carried out assuming a space group $R\bar{3}m$ with a α-$NaFeO_2$ type structure in which lithium is at the 3*b* site (0 0 1/2), transition metal ions at the 3*a* site (0 0 0), and oxygen at the 6*c* site (0 0 *z*). The hexagonal lattice parameters were obtained by least-squares fitting of the XRD data for compound I and from the Rietveld refined data for compounds II and III. The resulting values are I, $a = 2.884(7)$ Å, $c = 14.270(6)$ Å; II, $a = 2.876(5)$ Å, $c = 14.245(5)$ Å; and III, $a = 2.867(6)$ Å, $c = 14.224(7)$ Å. The

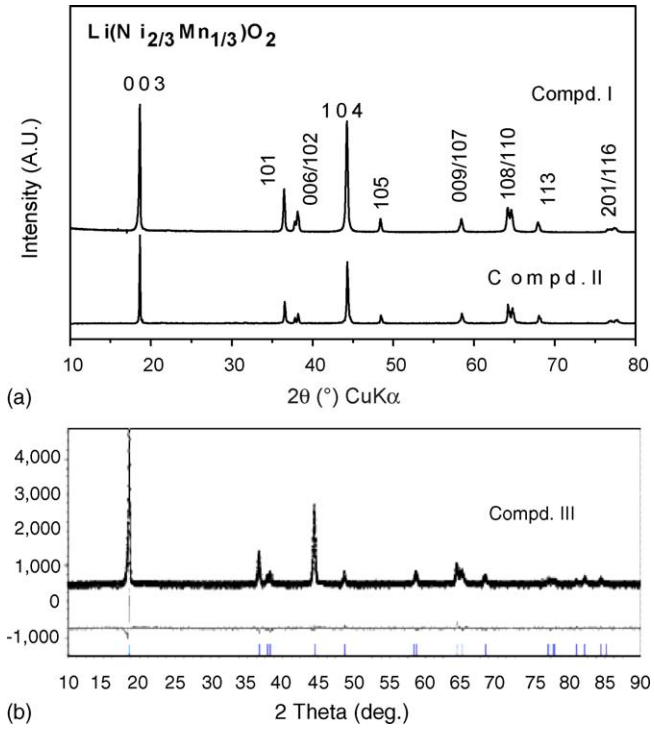

Fig. 1. X-ray diffraction patterns of $Li(Ni_{2/3}Mn_{1/3})O_2$ powders prepared by different methods: (a) compound I (freeze-drying) and compound II (carbonate method), Miller indices ($h\,k\,l$) are shown; and (b) compound III (molten salt synthesis). Circles and continuous lines represent experimental and fitted (Rietveld refined) X-ray diffraction patterns. The difference pattern is also shown. Vertical bars represent positions of allowed $h\,k\,l$ lines.

Rietveld refined parameters are II, $z = 0.247$, R-Bragg = 14.2, R(wp) = 25.5, goodness of fit (GoF) = 1.8; and III, $z = 0.264$, R-Bragg = 4.2, R(wp) = 6.45, GoF = 1.4. The observed and fitted XRD patterns for compound are found to be in good agreement, as shown in Fig. 1(b). During Rietveld refinement, 'cation-mixing' (i.e., site disorder through interchange of Li and Ni ions in the respective layers) was incorporated to maintain the total occupancy at unity. The 'cation-mixing' is about 10 and 4% for compounds II and III, respectively. The fairly low value of the cation-mixing in compound III (molten salt method) is understandable, given the presence of a large excess of Li-salts during its synthesis. The slight differences in the hexagonal lattice parameters of the three compounds are due to differences in cation-mixing during the respective method of synthesis. The a and c values match well with the $a = 2.88467$ Å and $c = 14.25943$ Å values reported by Kobayashi et al. [13] for $Li(Ni_{0.7}Mn_{0.3})O_2$. The c/a ratio of 4.95 and well-defined splitting of the XRD lines assigned to the pairs of Miller indices (0 0 6, 1 0 2) and (1 0 8, 1 1 0) are good indications of a well-ordered layer structure (Fig. 1) [3,7,13,14,18]. This is also reflected in the relative intensity ratio of the (0 0 3) and (1 0 4) lines in the XRD patterns, i.e., 1.2, 1.3 and 1.9 for compounds I, II and III, respectively.

Scanning electron micrographs (not shown) indicate agglomerates of sub-micron particles with platelet morphology for all three compounds. The size of the agglomerates ranges from 2 to 4 μm. The BET surface areas of powders are 3.9 and 2.8 (±0.1) $m^2\,g^{-1}$ for compounds I and II, respectively. These values are typical of oxide materials prepared at high temperature. The measured density of $Li(Ni_{2/3}Mn_{1/3})O_2$ (compound I) is 4.748 (±0.002) $g\,cm^{-3}$, which compares very well with the calculated X-ray density of 4.678 $g\,cm^{-3}$.

3.2. Cyclic voltammetry

Cyclic voltammograms (CVs) for cells with Li-metal as the counter and reference electrode were recorded at ambient temperature (25 °C) and at 50 °C, in the range 2.5–4.5 V, up to 30 cycles. Voltammograms at a fairly slow scan rate of 0.058 mV s^{-1} are presented in Fig. 2. For clarity, only selected cycles are shown. For compound I (freeze-drying method), the first-cycle anodic peak (extraction of Li-ions from the lattice) occurs at 4.10 V, whereas the main cathodic (insertion of Li) peak is at ~3.68 V. A minor cathodic peak (shoulder) at 4.2 V is also observed (Fig. 2(a)). During the second cycle, the anodic peak shifts to a lower potential (~4.0 V), but the corresponding cathodic peak is unaffected. The shift in the anodic peak is an indication of the 'formation' of the electrode in the first cycle, whereby the active material makes good electrical contact with the conducting carbon particles in the composite electrode, the Al-substrate and the liquid electrolyte. The hysteresis (ΔV = the difference between the fifth anodic and cathodic main peak potentials) is 0.27 V, which indicates good reversibility of the charge–discharge reaction. The ΔV remains almost constant on subsequent cycles, but the relative peak intensities (and area under the peak) decrease and a slight peak broadening occurs. This behaviour is due to capacity-fading. In addition, decreasing intensity of the anodic and cathodic peaks at 4.35 and 4.2 V, respectively, is clearly observed with the increasing cycle number. Almost identical CVs are displayed by compound II (carbonate method), as can be seen from Fig. 2(b). The ΔV value (0.18 V) on the sixth cycle is slightly smaller for compound II. Anodic and cathodic peaks in the region 4.2–4.35 V are also present in the CV of compound I recorded at 50 °C (Fig. 2(c)). The CV of compound III (molten salt synthesis) is similar to those of compounds I and II with respect to the potentials of the anodic and cathodic peaks. There are, however, minor differences, namely (i) the 'formation cycle' of the compound III is not completed until at least six cycles, as shown by a continuous shift in the peak potentials as well as by the changes in the general shape of the CV (Fig. 2(d)); and (ii) ΔV on the 12th cycle is 0.38 V, which is larger value than those shown by compounds I and II.

The anodic and cathodic peaks observed for $Li(Ni_{2/3}Mn_{1/3})O_2$ in the region 3.65–3.95 V can be attributed to the two-electron redox couple, $Ni^{2+/4+}$ in accordance with the assignment of the iso-structural compound, $Li(Ni_{1/2}Mn_{1/2})O_2$ [7–12]. It is noted, however, that the potential of the redox couple $Ni^{3+/4+}$ in the iso-structural compound $LiNi^{3+}O_2$ also lies in the 3.6–3.9 V range [1–3]. As shown by Ceder et al. [20,21], the potential of the redox couple of a transition metal ion such as Co^{3+} or Ni^{2+} is influenced by the presence of other ions (e.g., Al or Mn) in the crystal lattice. Due to strong interactions between

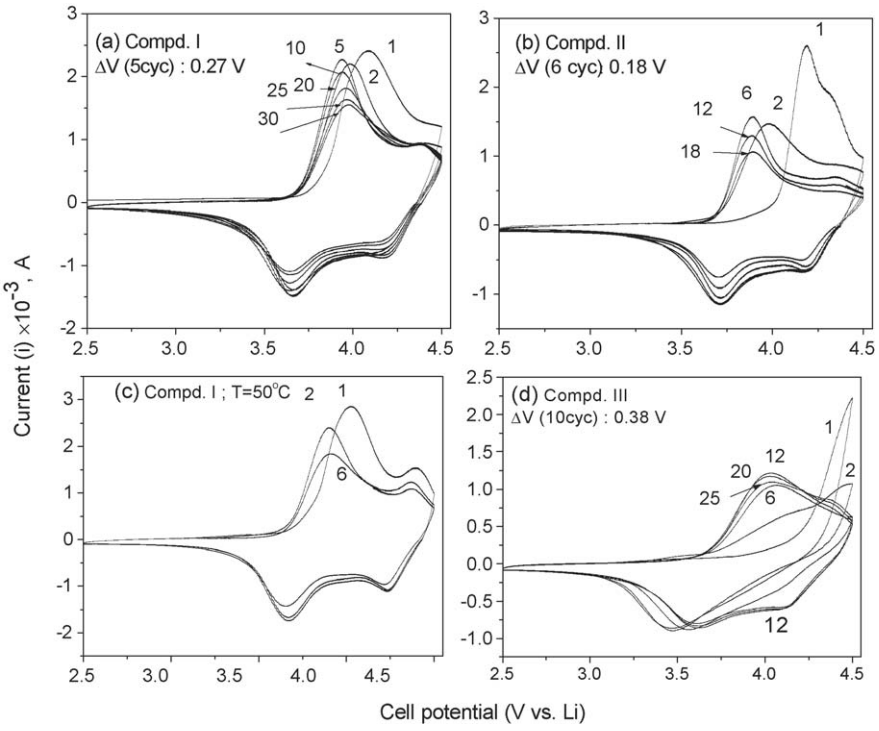

Fig. 2. Cyclic voltammograms (i–V curves) of $Li(Ni_{2/3}Mn_{1/3})O_2$: (a) compound I; (b) compound II; (c) compound I at $T = 50\,^{\circ}C$; and (d) compound III. Scan rate = 0.058 mV s^{-1}, at ambient temperature in voltage range 2.5–4.5 V. Number refers to cycle number.

the metal ions within the layers in the structure, the redox potential can either be shifted considerably from that encountered in the un-doped compound $LiCo^{3+}O_2$, or both $Ni^{2+/3+}$ and $Ni^{3+/4+}$ may exhibit almost identical redox voltages in the mixed oxide.

The origin of the minor anodic and cathodic peaks at ~4.35 and ~4.25 V, respectively, observed in the CVs is not clear at present. It possibly represents a reversible structural or order–disorder type of transition. It is noted that the areas under the peaks in the region 4.2–4.4 V are much smaller than those between 3.65 and 3.95 V, and thus cannot be due to the $Ni^{3+/4+}$ couple. Further, the anodic peak at ~4.35 V is not well-developed until at least six cycles in the ambient temperature CVs of all three compounds. On the other hand, both the anodic and cathodic peaks in the range 4.25–4.35 V are clearly evident in the CV of compound I recorded at 50 °C due to better Li-ion kinetics and the higher ionic conductivity of the electrolyte at the elevated temperature (Fig. 2(c)).

Cyclic voltammograms were also recorded for compound I at various scan rates (0.058–0.58 mV s^{-1}) at room temperature. As expected, the anodic and cathodic peak currents increase with the scan rate. A linear relationship is found between the anodic peak current and the square root of scan rate. By contrast, cathodic peak currents did not display linear behaviour at high scan rates (not shown). The voltage hysteresis (ΔV) versus (scan rate)$^{1/2}$ exhibited linear behaviour at all scan rates and is a typical characteristic of a solid-state, diffusion-controlled, lithium intercalation–deintercalation process. This feature has been observed for other cathodes, namely $LiCoO_2$ [18], $LiMn_2O_4$ [22], and $Li(Ni_{1/2}Mn_{1/2})O_2$ [12].

3.3. Charge–discharge cycling

Charge–discharge cycling of cells with $Li(Ni_{2/3}Mn_{1/3})O_2$ prepared by the above three methods, were carried out at ambient temperature for up to 80 cycles at a current density of 22 or 35 mA g^{-1} and with a lower cut-off voltage, 2.5 V versus Li. The upper cut-off voltage was 4.3 or 4.4 or 4.5 V. Selected voltage–capacity profiles for compounds I and III (freeze-drying and molten salt methods, respectively) are given in Fig. 3. The capacity versus cycle number plots for all three compounds are presented in Fig. 4. The open-circuit voltage (OCV) of all the fabricated and aged (24 h) cells is ~2.8 V. For all compounds, passage of current during the first charge causes a sudden increase in cell voltage to ~3.8–3.9 V, followed by a flat voltage profile up to a capacity of 25–35 mAh g^{-1}. Afterwards, the cell voltage gradually increased to the cut-off value. The first discharge and subsequent charge–discharge profiles are smoothly varying curves, typical of a single-phase Li-de-intercalation/intercalation reaction (Fig. 3). The initial capacities range from 190 to 240 mAh g^{-1} depending on the upper cut-off voltage, 4.3–4.5 V. There is an irreversible capacity loss (ICL) between the first discharge and charge that varies from 45 to 65 mAh g^{-1} according to the given compound and the upper cut-off voltage. This behaviour compares well with the initial charge capacity of 180 mAh g^{-1} and an ICL of 35 mAh g^{-1} observed by Kobayashi et al. [13] for the compound, $Li(Ni_{0.7}Mn_{0.3})O_2$. The 'formation' of the electrode and irreversible oxidation of Ni^{2+} ions trapped in the Li-layer (cation-mixing) during synthesis of the compounds are known to be some of the factors that contribute to ICL.

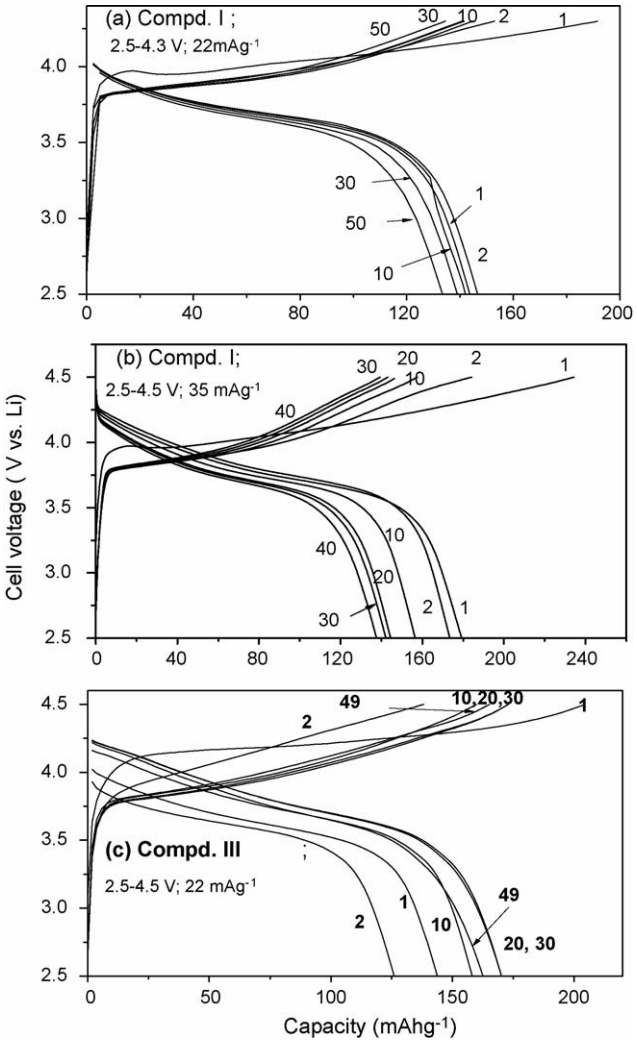

Fig. 3. Voltage vs. capacity profiles of $Li(Ni_{2/3}Mn_{1/3})O_2$: (a) compound I, 2.5–4.3 V, current 22 mA g^{-1}; (b) compound I, 2.5–4.5 V, current 35 mA g^{-1}; and (c) compound III, 2.5–4.5 V, current 22 mA g^{-1}. Numbers refer to cycle number.

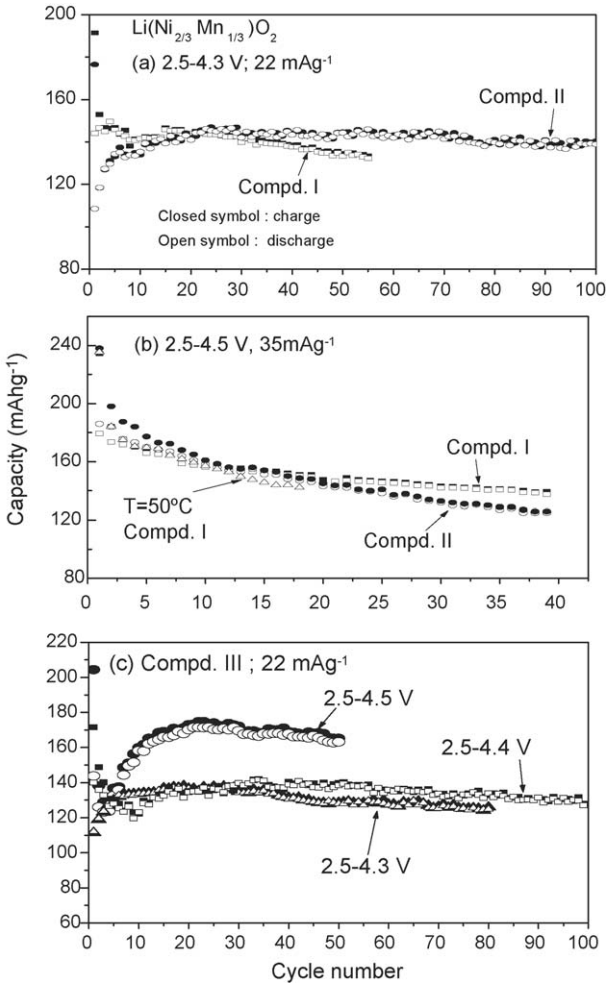

Fig. 4. Capacity vs. cycle number plots of $Li(Ni_{2/3}Mn_{1/3})O_2$: (a and b) compounds I and II; and (c) compound III. Voltage ranges and specific currents are indicated. Filled and open symbols represent charge and discharge capacities, respectively.

In the voltage range 2.5–4.3 V at a current density of 22 mA g^{-1} (0.15 C-rate, assuming 1C = 145 mA g^{-1}), compounds I and II yied capacities of 145 (±5) mAh g^{-1} during cycles 2–15. The coulombic efficiency (η, difference between charge and discharge capacity at any given cycle) is ≤95% (Figs. 3 and 4). This indicates that the 'formation' of the electrode is not complete up to 10–15 cycles, in accord with the observed CV data. During cycles 16–30, the capacities remain stable at 145 (±3) mAh g^{-1} and η increases to 98%. A small capacity fading occurs in compound I at the end of 55 cycles (95% retention). On other hand, the capacity of 145 (±3) mAh g^{-1} remains stable up to 100 cycles for compound II (carbonate method) (Fig. 4(a)). For compound III in the range 2.5–4.3 V at 22 mA g^{-1}, the capacity on the 20th cycle is 138 (±3) mAh g^{-1}.This remains stable up to 35 cycles but then slowly degrades to 128 (±3) mAh g^{-1} at the end of 80 cycles, i.e., 93% capacity retention (Fig. 4(c)).

When cycled in the range 2.5–4.5 V at 35 mA g^{-1}, the 10th cycle capacity of 160 (±3) mAh g^{-1} degrades by ∼10 and ∼20% at the end of the 40th cycle for compounds I and II, respectively. A similar trend in capacity fading is noted when compound I is cycled at 50 °C (Fig. 4(b)). The cycling behaviour of compound III shows that the 'formation' of the electrode is complete only after the initial 10–15 cycles. As can be seen in Fig. 4(c), during 15–50 cycles the capacity remains stable at 135 (±3) mAh g^{-1} in the voltage range 2.5–4.4 V at 22 mA g^{-1}. It degrades only slightly to 130 (±3) mAh g^{-1} at the end of 100 cycles, which corresponds to 96% capacity retention. When cycled in the range 2.5–4.5 V at 22 mA g^{-1}, the 20th cycle capacity of 170 (±3) mAh g^{-1} slowly degrades to 165 (±3) mAh g^{-1} after 50 cycles (97% retention). The slight differences in the cycling behaviour of $Li(Ni_{2/3}Mn_{1/3})O_2$ prepared by the three methods are due to variations in the crystallinity, morphology and cation-mixing that are known to govern the cathodic properties. Scope exists for capacity improvement and its retention by optimizing the synthesis conditions using the carbonate and molten salt routes.

The thermal stability of the cathode in the charged state (4.3 V) of compound I has been studied by differential scanning calorimetry (DSC) at a heating rate of 5 °C min^{-1}. The

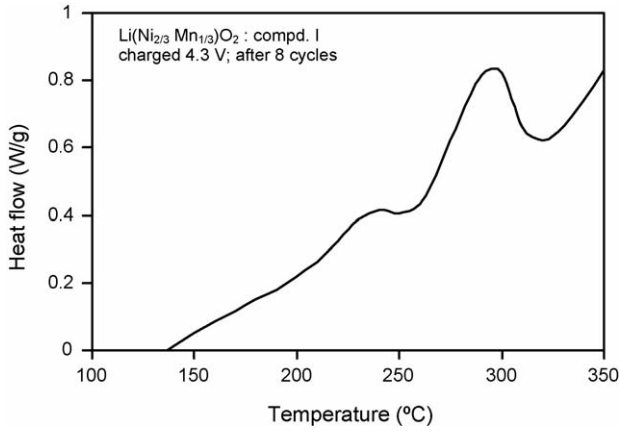

Fig. 5. DSC curve of charged-electrode (4.3 V) of compound I after eight cycles. *Y*-axis normalized with respect to weight of active material. Heating rate = 5 °C min^{-1}.

electrode has been recovered after dismantling the cell in the glove box (after eight cycles). The heat flow values (*Y*-axis) have been normalized with respect to the active mass of cathode. The characteristic exothermic peak (T_d) due to destruction of the structure and oxygen evolution is observed at 295 (±2) °C (Fig. 5). There is also a minor exothermic peak at 235 (±2) °C. The T_d of 295 °C compares well with the T_d reported for the similar compounds $Li(Co_{1-2x}Ni_xMn_x)O_2$, $0.25 \leq x \leq 0.5$ [23], but is much higher than that for $Li_{0.5}CoO_2$ (230–250 °C) [24,25] and $Li_{0.5}NiO_2$ (220 °C) [25].

4. Conclusions

The compound $Li(Ni_{2/3}Mn_{1/3})O_2$ with a layer structure is prepared by means of the freeze-drying, mixed carbonate and molten salt methods. The phases are characterized by powder XRD, SEM, BET and density methods and are tested for cathodic behaviour in cells with Li-metal as a counter electrode. Cyclic voltammetry shows redox processes at 3.6–4.0 V corresponding to the $Ni^{2+/3+}$–$Ni^{3+/4+}$redox couple. Galvanostatic charge–discharge cycling is carried out at 22 or 35 mA g^{-1} with upper cut-off voltages of 4.3, 4.4 or 4.5 V. The lower cut-off voltage is 2.5 V. Compound II (carbonate method) shows a stable capacity of 145 (±3) mAh g^{-1} up to 100 cycles in the voltage range 2.5–4.3 V at 22 mA g^{-1} without any noticeable fading. Compound III (molten salt method) exhibits a stable capacity of 135 (±3) mAh g^{-1} up to 50 cycles in the voltage range 2.5–4.4 V at 22 mA g^{-1}, and retains 96% capacity after 100 cycles. The performance of compound I (freeze-drying method) is slightly inferior to that of compounds II and III. Higher reversible capacities of 160–170 mAh g^{-1} are obtained on cycling in the range 2.5–4.5 V at 22 or 35 mA g^{-1}, but capacity fading is noted at the end of 50 cycles for all the compounds. The DSC data of the charged electrode of compound I (to 4.3 V) reveals that the decomposition temperature is 295 (±2) °C, which compares well with the values noted for compounds, $Li(Co_{1-2x}Ni_xMn_x)O_2$, $x = 0.25$–0.50.

References

[1] W.A. Van Schalkwijk, B. Scrosati (Eds.), Advances in Lithium-Ion Batteries, Kluwar Acad./Plenum Publ, New York, USA, 2002.
[2] G.-A. Nazri, G. Pistoia (Eds.), Lithium Batteries: Science and Technology, Kluwer Acad. Publ, USA, 2003.
[3] E. Rossen, C.D.W. Jones, J.R. Dahn, Solid State Ionics 57 (1992) 311.
[4] Y. Nitta, K. Okamura, K. Haraguchi, S. Kobayashi, A.O. Ohta, J. Power Sources 54 (1995) 511.
[5] M.E. Spahr, P. Novak, B. Schnyder, O. Haas, R. Nesper, J. Electrochem. Soc. 145 (1998) 1113.
[6] Z. Lu, L.Y. Beaulieu, R.A. Donaberger, C.L. Thomas, J.R. Dahn, J. Electrochem. Soc. 149 (2002) A778.
[7] Y. Makimura, T. Ohzuku, J. Power Sources 119–121 (2003) 156.
[8] K.M. Shaju, G.V. Subba Rao, B.V.R. Chowdari, Electrochim. Acta 48 (2003) 1505.
[9] C.S. Johnson, J.-S. Kim, C. Lefief, N. Li, J.T. Vaughey, M.M. Thackeray, Electrochem. Commun. 6 (2004) 1085.
[10] S.-H. Na, H.-S. Kim, S.-I. Moon, Electrochim. Acta 50 (2004) 447.
[11] O.A. Shlyakhtin, Y.S. Yoon, S.H. Choi, Y.-J. Oh, Electrochim. Acta 50 (2004) 503.
[12] M.V. Reddy, G.V. Subba Rao, B.V.R. Chowdari, Electrochim. Acta 50 (2005) 3375.
[13] H. Kobayashi, H. Sakaebe, H. Kageyama, K. Tatsumi, Y. Arachi, T. Kamiyama, J. Mater. Chem. 13 (2003) 590.
[14] K.S. Tan, M.V. Reddy, G.V. Subba Rao, B.V.R. Chowdari, J. Power Sources 141 (2005) 129.
[15] X. Yang, W. Tang, H. Kanoh, K. Ooi, J. Mater. Chem. 9 (1999) 2683.
[16] H. Liang, X. Qiu, S. Zhang, Z. He, W. Zhu, L. Chen, Electrochem. Commun. 6 (2004) 505.
[17] C.-H. Han, Y.-S. Hong, K. Kim, Solid State Ionics 159 (2003) 241.
[18] K.S. Tan, M.V. Reddy, G.V. Subba Rao, B.V.R. Chowdari, J. Power Sources 147 (2005) 241.
[19] K.M. Shaju, G.V. Subba Rao, B.V.R. Chowdari, Electrochem. Commun. 4 (2002) 633.
[20] G. Ceder, Y.-M. Chiang, D.R. Sadoway, M.K. Aydinol, Y.-I. Jang, B. Huang, Nature 392 (1998) 694.
[21] J. Reed, G. Ceder, Electrochem. Solid-State Lett. 5 (2002) A145.
[22] K.A. Striebel, A. Rougier, C.R. Horne, R.P. Reade, E.J. Carins, J. Electrochem. Soc. 146 (1999) 4339.
[23] D.D. MacNeil, Z. Lu, J.R. Dahn, J. Electrochem. Soc. 149 (2002) A1332.
[24] Y. Baba, S. Okada, J.-I. Yamaki, Solid State Ionics 148 (2002) 311.
[25] Z. Zhang, D. Fouchard, J.R. Rea, J. Power Sources 70 (1998) 16.